

Article

The Influence of Animal Glue as an Additive on the Properties of Lime Architectural Grouts

Andreja Padovnik * and Violeta Bokan-Bosiljkov

Faculty of Civil and Geodetic Engineering, University of Ljubljana, Jamova 2, SI-1000 Ljubljana, Slovenia; violeta.bokan-bosiljkov@fgg.uni-lj.si

* Correspondence: andreja.padovnik@fgg.uni-lj.si

Abstract: Organic additives from plant and animal extracts were commonly used in lime mortar in the past to improve and modify its properties. In modern times, they have been replaced by inorganic additives. The objective of this research is to investigate the influence of fish animal glue and the role of the filler particle size distribution on the fresh and hardened properties and durability of lime grouts. Wet density, water retention, fluidity, and injectability were tested in the fresh state. It was found that the particle size distribution of the selected filler, which can increase the packing density of the solid particles of the grout, and the W/B ratio have a great influence on water retention and fluidity. In the hardened state, porosity and compressive and splitting tensile strength were evaluated on 90-day- and 365-day-old specimens. The presence of animal glue improved the mechanical properties, due to a higher carbonation rate. The combination of the two fillers that resulted in a better packing of filler particles decreased the splitting tensile strength of the grout. To investigate the durability of the selected grouts, adhesion strength was measured on disc-sandwich models after non-accelerated and accelerated aging. The results show that the adhesive strength of grouts aged under laboratory conditions is lower than that of grouts subjected to accelerated aging.

Keywords: architectural injection grout; dry hydrated lime; organic additive; animal glue; mechanical properties; durability



Citation: Padovnik, A.; Bokan-Bosiljkov, V. The Influence of Animal Glue as an Additive on the Properties of Lime Architectural Grouts. *Sustainability* **2023**, *15*, 12903. <https://doi.org/10.3390/su151712903>

Academic Editor: Antonio Caggiano

Received: 30 June 2023

Revised: 10 August 2023

Accepted: 22 August 2023

Published: 25 August 2023



Copyright: © 2023 by the authors. Licensee MDPI, Basel, Switzerland. This article is an open access article distributed under the terms and conditions of the Creative Commons Attribution (CC BY) license (<https://creativecommons.org/licenses/by/4.0/>).

1. Introduction

Injection grouts based on lime binders for stabilizing detached decorative plaster layers have been intensively tested by researchers in recent years [1–6]. Most injection grouts are based on a lime binder that fulfils the aspect of compatibility with original lime-based decorative plasters. In addition to the lime binder, these lime-based grouts also contain fillers, water, and additives that improve workability and/or increase mechanical properties and durability in the hardened state.

An additive is defined as a constituent that is added to the binder, usually in a small amount of at least 1% weight/weight (w/w), to modify its preparation or its properties in the fresh/hardened state, and it is a substance other than the binder, aggregate, filler, or water [7]. The use of organic additives in lime mortars dates back to Greek and Roman times [8]. The list of traditional organic additives used in Europe since the last century BC was compiled by Sickels [9]. Organic additives from plant and animal extracts such as lipids, carbohydrates, and proteins were commonly used in lime mortars in the past to improve and modify their properties [9]. In modern times, these traditional organic additives have been replaced by commercial additives such as resins and synthetic organic materials. Thus, little knowledge about traditional organic additives has been preserved to date.

In recent decades, very little research has been done on lime mortars and injection grouts with traditional organic additives. In their study, Pasian et al. [4] investigated the effects of two water-reducing components, ethanol and ovalbumin protein, a natural

water-reducing and air-entraining additive, on lime-based injection grouts. The main conclusion of their study [4,10] was that ovalbumin affects the carbonation and pozzolanic reaction rates, which increase porosity and consequently reduce mechanical strength. Papayianni et al. [11] also developed an injection grout based on hydrated lime, natural pozzolan, and two additives, such as a polycarboxylate superplasticizer and linseed oil, to improve the adhesion and hydrophobicity of the grout. The results showed [11] that 1% *w/w* of linseed oil in the lime pozzolan grout helped to maintain viscosity for a longer period of time, increased penetrability, and decreased compressive strength. However, when the grout was tested as a cubic, ground-sand specimen, the compressive strength increased, indicating that the use of linseed oil improves the coherence ability of the grout mixture [11].

In addition, the influence of traditional organic additives on the physical and mechanical properties of lime mortars has also been studied [7,12–15]. Ventolà et al. [12] found that organic additives such as animal-bone glue, nopal, casein, and olive oil in lime mortars improved the mechanical properties and reduced porosity, and nopal also increased the carbonation rate. Similar conclusions were drawn from the studies in [14], according to which an organic additive prepared from *Ficus carica* fruit in combination with the suitable grain size distribution of river sand improved the carbonation rate and mechanical properties of lime mortars. Furthermore, fermented red grapes as an additive in lime mortars contributed to the carbonation speed of lime mortars, which resulted in a higher mechanical strength of mortars [16]. In contrast to these results, Elert et al. [13] found that the presence of animal glue (rabbit-skin glue) affected the mineralogical evolution, weathering resistance, and mechanical strength of lime plasters. The main conclusion is that the degree of carbonation decreases with the increasing content of organic animal glue in lime plasters, and consequently, the flexural and compressive strength decreases.

It has been shown that the presence of traditional organic additives can affect the carbonation and hydraulic reactions in lime mortars and improves their mechanical properties [7]. Organic additives, such as hygroscopic animal glue, act as a moisture retainer and slow down the drying process, so that the carbonation process is facilitated by water and proceeds according to the following reaction (1) [13,14]:



In addition, the properties of lime grout can also be improved by changing the particle size distribution of the filler. The design of concrete, for example, is based on the optimal packing of granular particles, which can improve the fresh and hardened properties of the material. Jayasingh et al. [14] showed that the effective particle size distribution can influence the carbonation process so that the modification of the pore system affects the diffusion of CO_2 in the mortar. The influence of the particle size distribution of sand in lime mortar has been studied by many researchers [14,17–19].

In this research, a fish glue solution was used as an organic additive in lime architectural grout to increase the cohesiveness of the grout in the fresh state. In addition to the organic additive, three fillers with different particle size distributions were selected to study their effects on the properties of the grout. The influence of these modifications to the lime grout composition was studied on fresh and hardened specimens. In the hardened state, the porosity and mechanical properties were analyzed at the age of 90 days and over a longer period of 365 days. To evaluate the durability of the detached plaster layer stabilization, the grouts were injected into a sandwich disc, simulating an air pocket between two plaster layers, cured for 365 days, and after that, they were subjected to accelerated aging by freezing–thawing and heating–cooling cycles.

2. Materials and Methods

In this study, several grout mixtures of lime, filler, and water with or without organic additives were prepared. The compositions of the tested grout mixtures are listed in Table 1. Commercial dry hydrated lime type CL 70-S [20] (IAK, Kresnice, Slovenia) was used as

a binder. Three commercially available finely ground limestones (F40, F15, and F5) from Slovenia (CALCIT, Stahovica, Slovenia) were used as fillers. The chemical composition of the lime and filler, determined by X-ray fluorescence analysis [21] (Bruker S8 TIGER, Anhovo, Slovenia) is presented in Table 2. The crystalline phases in the binder and filler were analyzed by X-ray powder diffraction (XPert Pro X-ray diffractometer; measurement parameters: Cu-K α radiation $\lambda = 1.54 \text{ \AA}$, exploration range from 20° to 70° 2θ , University of Ljubljana, Faculty of Chemistry and Chemical Technology, Slovenia) and are presented in Table 3. The Rietveld method was used for the quantitative phase analysis of the samples.

Table 1. Composition of grout mixtures.

Mixture ID	Binder/Filler Mass Ratio	Limestone Filler F40:F15:F5 Mass Ratio	Water/Binder Mass Ratio	Water/(Binder, Limestone Fillers) Mass Ratio	PCE (%)	Animal Glue (%)
LS	0.28	0:100:0	1.86	0.41	0.5	-
LS-G1	0.28	0:100:0	1.86	0.41	0.5	0.34
LS-G2	0.28	0:100:0	1.76	0.39	0.5	0.34
LF	0.28	70:0:30	1.86	0.41	0.5	-
LF-G1	0.28	70:0:30	1.86	0.41	0.5	0.34
LF-G2	0.28	70:0:30	1.80	0.40	0.5	0.34

Table 2. XRF composition of the lime type CL 70-S and limestone fillers (F40, F15, and F5).

Sample	CaO (%)	MgO (%)	Al ₂ O ₃ (%)	Fe ₂ O ₃ (%)	SO ₃ (%)	SiO ₂ (%)	I.L. (%)
CL 70-S	71.25	2.09	0.60	0.19	0.06	0.79	25.69
Limestone filler (F40, F15 and F5)	55.38	0.76	0.15	0.01	0.01	<0.01	44.02

Table 3. Contents of the crystalline phases for lime and limestone fillers, obtained by the Rietveld method.

Sample	Portlandite (Ca(OH) ₂)	Calcite (CaCO ₃)	Periclase (MgO)	Magnesite MgCO ₄	Larnite (Ca ₂ SiO ₄)	Dolomite (CaMg(CO ₃) ₂)
CL 70-S	95.8	2.9	0.2	0.3	0.8	
Limestone filler (F40, F15 and F5)		95.3				4.7

The results in Tables 2 and 3 show that the lime can be characterized as a high-calcium lime (Ca(OH)₂ $\geq 90\%$) with a small amount of CaCO₃ ($\leq 6\%$ by mass). The chemical composition of all three limestone fillers (F40, F5, and F15) is the same and consists of a very pure calcite powder, which is 95.3% calcite and 4.7% dolomite (Table 3).

The particles of the limestone fillers (F40, F15, and F5) have a density of 2.76 g/cm³. The main difference between the limestone fillers is the particle size distribution (Table 4). The coarsest-grained limestone filler is F40, with a maximum size of 120 μm , and the finest is F5, with a maximum size of 12 μm (Table 4).

Table 4. Grain size distribution of the limestone fillers F40, F15, and F5.

Type of Limestone Filler	Particle Size				
	Maximum Size	Cumulative 10%	Cumulative 20%	Cumulative 50%	Cumulative 90%
F40	120 μm	3 μm	8 μm	16 μm	60 μm
F15	100 μm	3 μm	9 μm	15 μm	40 μm
F5	12 μm	0.8 μm	1.5 μm	4.5 μm	11.5 μm

For the preparation of the grout mixtures, two additives were used, which were selected by some preliminary tests.

A polycarboxylate ether-based superplasticizer, PCE (0.5% by mass of the binder and filler), with a relative density of 1.05 g/cm^3 and a pH of 5.5 ± 1.0 (TKK, Srpenica, Slovenia) was used to reduce the water content but maintain the adequate workability of the grouts [2].

The second additive was a natural polymer derived from fish collagen with adhesive properties [22]. The purest form of fish glue is so-called isinglass, which is obtained from the skins of non-oily fish species or their bones, heated in water, then cooled and dried to produce gelatin or glue.

The fish glue product selected is a liquid solution with a water content of approximately 55%, a relative density of 1.17 g/cm^3 , and a pH value of 6 (Deffner & Johann, Röthlein, Germany) [23]. Figure 1 shows the transmission ATR-FTIR spectra of pure protein fish glue, recorded with a Spectrum 100 spectrometer (PerkinElmer, Shelton, CT, USA). The sample was averaged based on 16 scans in the spectral range from 4000 cm^{-1} to 500 cm^{-1} with a resolution of 4 cm^{-1} . The 32-bit software OPUS 8.1 (BrukerOptik GmbH) was used to analyze the obtained spectra. The typical absorption band in the range of $3400\text{--}3200 \text{ cm}^{-1}$ for the amino group is a characteristic stretching vibration of the N-H band. The band at 2942 cm^{-1} is due to the characteristic C-H stretching and can be attributed to the organic binder. The fingerprints of the proteins are clearly seen from the characteristic absorption peaks: amide I C=O stretching vibration at 1630 cm^{-1} ; amide II C-N stretching vibration and N-H bending vibration at 1519 cm^{-1} ; and amide III C-H bending vibration at 1442 cm^{-1} [24].

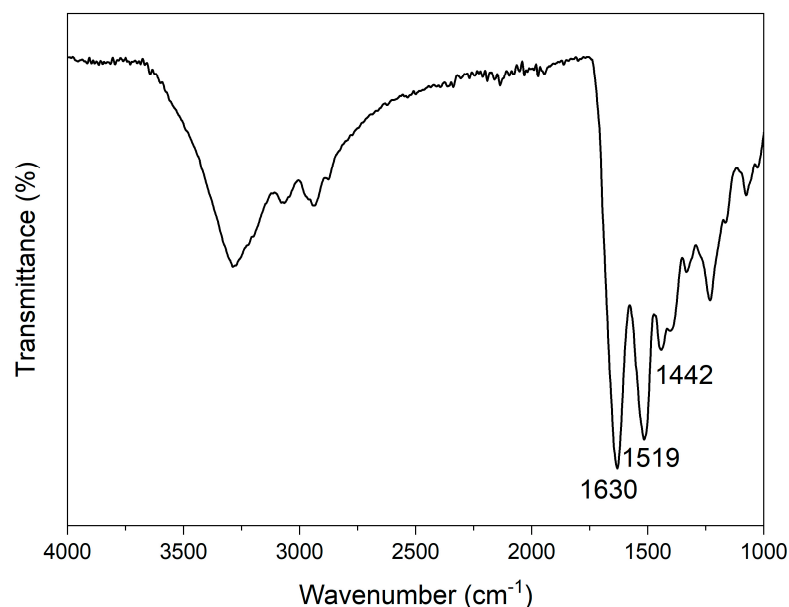


Figure 1. ATR-FTIR spectra of pure fish glue.

The selected binder/filler ratio was 0.28 by mass. This decision was made in accordance with previous data [1]. Six different grout mixtures were prepared (Table 4), which were divided into two groups (Figure 2). In both groups, a reference grout mixture (LS and LF) was prepared without organic additives. The main difference between the two groups is the type of filler. In the first group (LS, LS-G1, and LS-G2), only the F15 limestone filler was used according to previous studies [1]. In contrast, in the second group (LS-F, LS-F-G1, and LS-F-G2), the fillers F40 and F5 were mixed in a ratio of 70:30. The proposed ratio of the F40 and F5 fillers was chosen based on preliminary studies where the stability and injectability of the grout were the parameters studied.

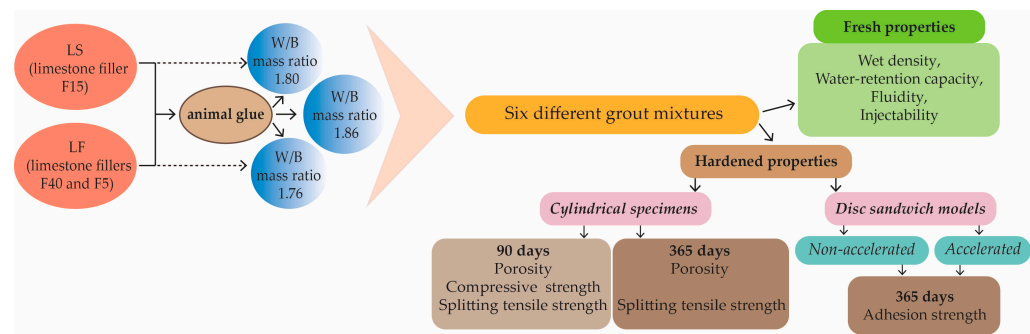


Figure 2. Flowchart of research progress.

The liquid animal glue additive was incorporated into each of the remaining grouts, at a dosage of 0.34%, calculated as a percentage of the total weight of the binder. This dosage of 0.34% was enough to obtain an adequate cohesion of the lime grout in the injectability test (grout effectively binds the quartz sand grains together). To prevent the formation of molds after the grout application, the animal glue dosage was kept as low as possible.

Three parameters of the references grout mixtures remained unchanged in the remaining grout compositions; the hydrated lime, filler content, and the PCE dosage. The water content of the mixtures was adjusted to achieve an adequate workability of the grouts. The grouts were prepared with tap water.

A KitchenAid mixer (power 300 W) with a stainless-steel gate anchor blade was used to mix the grouts. First, the binder and the filler were mixed. Then, 70% of the water and animal glue were added and mixed for 3 min at low speed (540 rpm). In the last 15 s of the slow mixing, the PCE and 30% of the water were added. Mixing continued at medium speed (1200 rpm) for 3 min.

The properties of the grouts in fresh and hardened states (Figure 2) were evaluated using the guidelines proposed by Biçer-Şimşir and Rainer [6] or Padovnik and Bosiljkov [1]. For each grout mixture, at least three repetitions of each test were performed.

The wet density of grout was analyzed according to the modified standard method EN 1015-6 [25]. The volume of the grout was reduced from 1000 mL to 10 mL [6].

According to the standard prEN 1015-8 [26], the water-retention capacity of the grouts was investigated.

Fluidity by means of a flow cone was performed according to the modified standard method EN 445 [27]. Measurements of 1000 mL of grout were taken immediately after mixing.

The injectability test was performed based on the standard procedure EN 1771 [28] (Figure 3). Dry siliceous sand with a grain size between 2 and 4 mm was used as the granular material, simulating around a 0.3–0.6 mm large crack or void width.

Two sets of samples were prepared to evaluate the hardened properties (Figures 2 and 4): (I) For the mechanical and physical tests, cylindrical molds of 50/50 mm size were made to cast at least three specimens for each property and age. After 48 h, they were removed from the molds and cured under controlled environmental conditions (RH 55 ± 5% and 20 ± 1 °C) for 90 and 365 days. The mechanical and physical properties of the grouts were determined at the age of 90 days, and the splitting tensile strength and porosity were measured again after 365 days.

The total and capillary porosity were assessed according to the Swiss standard SIA 262/1:2008 [29].

Compressive and splitting tensile tests were performed according to the standard EN 1015-11 [30] and the ASTM C496/C496M-11 method [31], respectively. The Roel Amsler HA 100 servo-hydraulic testing machine (Zwick GmbH & Co. KG, Ulm, Germany) was used to measure the compressive and splitting tensile strengths, supplemented with a load cell with the capacity adjusted to the compressive (25 kN) and splitting tensile (5 kN) strength of the tested specimens.

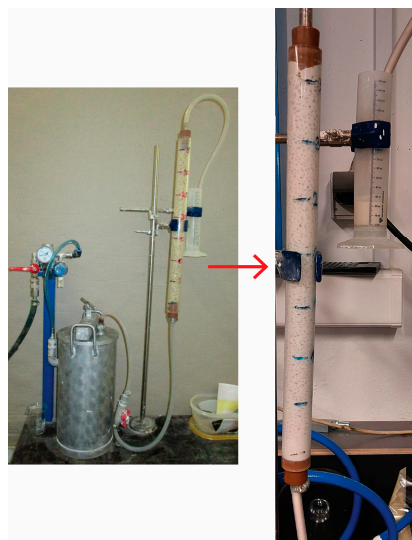


Figure 3. Injectability apparatus with the column filled with dry siliceous sand (left) and the column after the injectability test (right).



(a)



(b)

Figure 4. Two sets of specimens were prepared to evaluate the hardened properties: (a) cylindrical specimens; (b) disc-sandwich model specimens.

(II) To evaluate the adhesion strength and durability of the grout, a pull-off test was performed on disc-sandwich models [32] according to the standard EN 1015-12 [33]. The models were prepared according to the instructions [32] and simulated 2 mm- and 5 mm-high air pockets between the fine plaster (1 part lime putty and 3 parts fine limestone sand 0/1 mm) and the coarse plaster (1 part lime putty and 3 parts coarse limestone sand 0/4 mm). The disc-sandwich models simulating air pockets were injected with the grout at the age of 1 year using a syringe. The Proceq pull-off tester DY-206 with a working range of 0.3 to 3.1 MPa (0.6 to 6 kN for the 50 mm test disc/pull-head) was used to apply the tensile load to the test surface.

At the age of 1 year, adhesion strength was measured on the non-accelerated and accelerated disc-sandwich models.

To analyze the durability of the grouts, accelerated aging was performed on the injected disc-sandwich models. The models were subjected to ten freezing–thawing and heating–cooling cycles, according to the protocol in [1]. Prior to each cycle, the discs were subjected to capillary absorption of 3% NaCl solution for 30 min (Figure 5), according to the RILEM test No. II.6 [34].



Figure 5. Sandwich discs exposed to capillary absorption of 3% NaCl solution.

3. Results and Discussion

3.1. Wet Density, Water-Retention Capacity, Fluidity, and Injectability

Table 5 shows the average values of the wet density, water-retention capacity, and fluidity of the tested grouts. There are no significant differences between the fresh properties. The wet density, 1.74 g/cm^3 , is the same for grouts LS, LS-G1, LF, and LF-G1 with the same water/binder (W/B) mass ratio (Table 4). It can also be seen that different limestone fillers have no effect on the wet density, as the particle density of the fillers is the same (Table 3). As expected, grouts LS-G2 and LF-G2 with a lower water/binder ratio (Table 4) have a higher wet density, up to 1%, compared to the grouts with 1.74 g/cm^3 .

Table 5. Fresh grout properties.

Mixture ID	Wet Density of Fresh Grout (g/cm^3)	Water-Retention Capacity (%)	Fluidity (s)
LS	1.74 ± 0.05	83 ± 1	29 ± 3
LS-G1	1.74 ± 0.01	83 ± 2	27 ± 2
LS-G2	1.76 ± 0.01	87 ± 1	40 ± 3
LF	1.74 ± 0.01	85 ± 1	25 ± 1
LF-G1	1.74 ± 0.01	85 ± 1	25 ± 2
LF-G2	1.75 ± 0.02	86 ± 2	49 ± 3

For all tested grouts, the average values for water retention range from 83% to 87% (Table 5). Higher water-retention capacities of 87% and 86% are obtained for grouts LS-G2 and LF-G2, respectively, with a lower W/B ratio (Table 4). The results show that the type of filler can have a significant effect on the packing density of the solid particles of the grout. The combination of fillers F40 and F5 increases the water-retention capacity of grouts LF and LF-G1, in contrast to grouts LS and LS-G1 with filler F15. Because of its high-water retention capacity, the grout resists the release of water into the highly porous media through which it flows. In this way, the injection of the grout between detached plasters can be improved, and its drying shrinkage can be effectively reduced [6]. The higher water-retention capacity of grouts LF and LF-G1 with the combination of two fillers F40 and F5 could be due to a lower free-water content.

In our previous study [1], it was shown that the filler with a suitable grain size composition can optimally fill the voids within the grout matrix. Consequently, less free water would be available in the grout during the suction action of the porous plaster, and bound water cannot be easily removed [35].

Furthermore, if we compare grouts LS and LF with grouts LS-G1 and LF-G1, we find that the animal glue in grouts LS-G1 and LF-G1 had no effect on the water-retention capacity.

Regarding fluidity, the average values for 1000 mL of the tested grouts ranged from 25 to 49 s (Table 5). Again, the influence of the W/B ratio and the type of filler is obvious. Grouts LS-G2 and LF-G2 with a lower W/B ratio also showed higher values with 40 and 49 s, respectively, than the reference grouts LS and LF with 29 and 25 s, respectively. As already mentioned, the type of filler influences fluidity. The combination of fillers F40 and F5 proved to be more effective compared to the grout with filler F15. On the other hand, the average flow time of grout LS-G1 with animal glue is lower (27 s) compared to the reference grout LS. However, the average flow time is the same for grouts LF and LF-G1 with 25 s.

The injectability curve of the tested grouts is shown in Figure 6 for dry siliceous sand columns. According to the results, the reference grouts LS and LF reached 350 mm in 150 s and also filled an additional 20 mL graduated cylinder, which is considered excess grout and is marked in the graph as an additional data point at 370 mm [6]. Comparing the injectability curves of grouts LS and LF, it can be seen that grout LF with the combination of two fillers (F40 and F5) reduces the injectability in the initial phase by up to 350 mm compared to the reference grout LS.

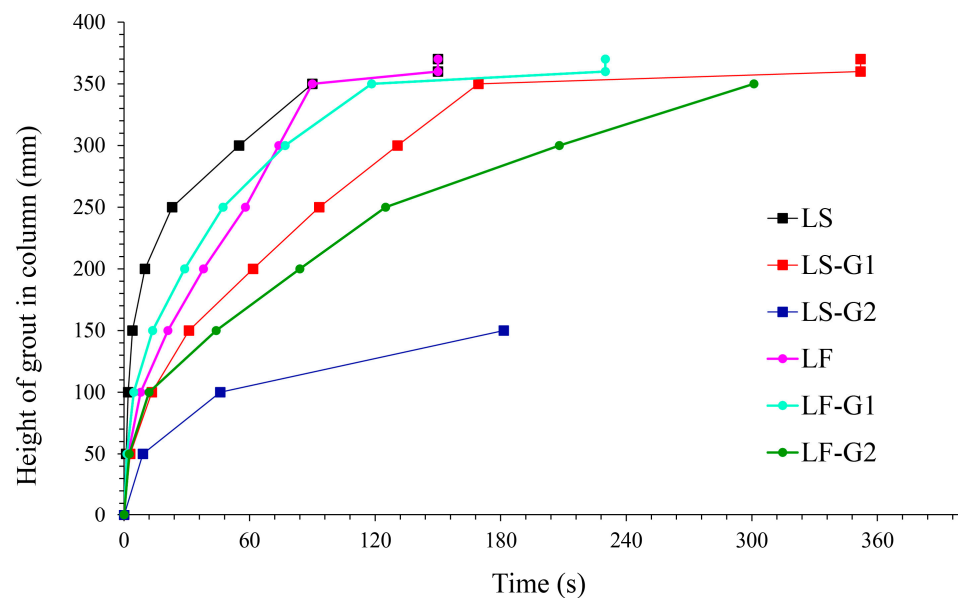


Figure 6. Injectability curves of the grouts for dry siliceous sand columns.

The results also show the effects of animal glue and W/B ratio on the ability to fill the dry siliceous sand columns with grout. The W/B ratio has a great influence not only on injectability but also on fluidity. The worst injectable grout is LS-G2, with the lowest W/B ratio (Table 4). In the case of the grouts with the animal glue addition, the injectability of the grouts decreases compared to the reference grouts LS and LF. Moreover, the combination of two fillers and animal glue (LF-G1) increases injectability compared to the grout LS-G1 with filler F15 and animal glue. The obtained results are not consistent with those of the study carried out by Sickels [9], where it is reported that animal glue increases workability. On the other hand, the study by Schellmann [22] states that animal glue may have an undesirable tendency to form small air bubbles in the glue matrix. The same effect, that animal glue acts as a foaming agent, was also noted by Elert et al. [13]. During the mixing of grouts with animal glue, we noticed some air bubbles, especially when a high speed was used. These air bubbles in grouts with animal glue may reduce injectability.

3.2. Porosity

The total and capillary porosity of 90-day-old grout samples and the porosity of the same samples after 365 days are shown in Figure 7. The total porosity of all grouts at the age of 90 days is in a narrow range between 41.1 and 43.0%, despite the different B/W

ratios, different fillers, and added organic additive. The combination of different fillers in the grouts has no significant effect on the total and capillary porosity. Grouts LF, LF-G1, and LF-G2 with the combination of two fillers have a total porosity of 42.0% and a capillary porosity of 38.0%. The lowest values of total porosity and capillary porosity were obtained for grout LS-G2 with a lower W/B ratio (41.1 and 35.5%, respectively).

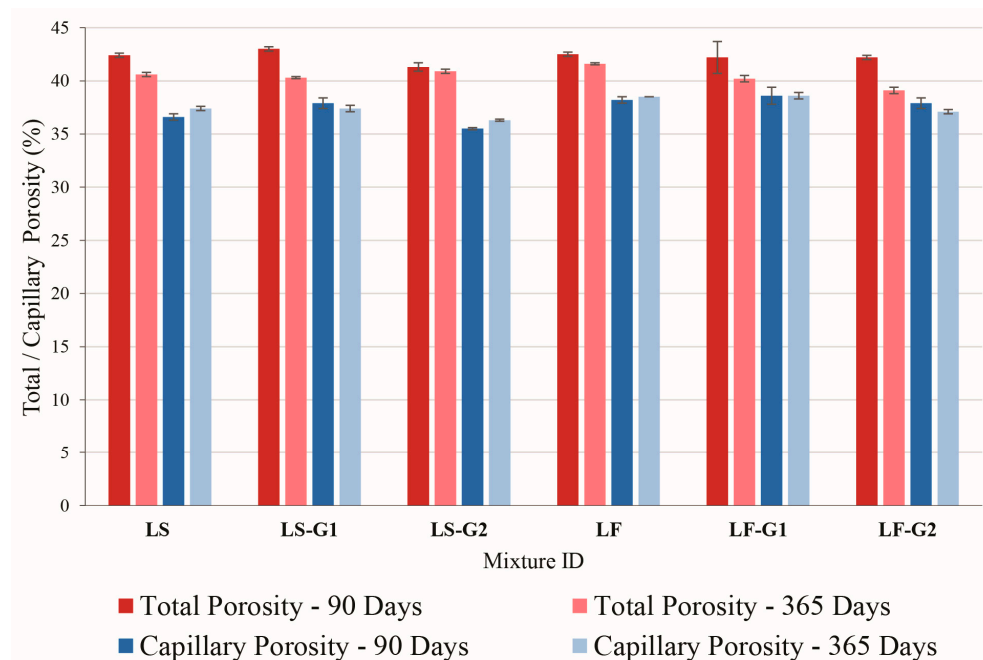


Figure 7. Total and capillary porosity at 90 and 365 days.

The results obtained for grouts LS and LS-G1 at the age of 90 days are of the same trend as in the study on lime plasters with animal glue [13], where the addition of animal glue led to a significant change in the pore size distribution. In the study [13], it was shown that the higher the content of organic additives, the higher the total porosity and the number of pores with a diameter greater than $>2 \mu\text{m}$. Elert et al. [13] also report that the larger, irregularly shaped air voids in the plaster are due to the foaming effect of the animal glue, which makes homogeneous mixing of the filler and hydrated lime powder difficult. Thus, the increase in the total porosity of the LS-G1 composition may be due to the increased air bubble content in the fresh grout as a result of the animal glue addition.

After 365 days, total and capillary porosity were measured again on the same specimens that had been measured after 90 days. In all grout specimens, the total and capillary porosity decreased by up to 15% and 3%, respectively, compared to the 90-day-old samples.

These results suggest that after 356 days, animal glue in the grout has a positive effect on the carbonation rate, as it is slightly higher (LS-G1, LF-G1, and LF-G2) than in grouts without organic additives. Elert et al. [13] attributed this phenomenon to the hygroscopic animal glue, which acted as a moisture retainer in the grouts and slowed down the drying process. This facilitated the carbonation process due to the required water [13], during the long period. The same observation was made by Walker and Pavia [36], namely that water retainers have a positive effect on the carbonation reaction.

3.3. Compressive and Splitting Tensile Strength

The average values for the mechanical strengths with corresponding standard deviation are shown in Table 6. A lower W/B ratio increases the compressive and splitting tensile strength of grouts LS-G2 and LF-G2 compared to the reference grouts LS and LF, which is also consistent with porosity (Figure 7). Moreover, it is not evident from the results that different fillers can improve compressive strength.

Table 6. Compressive and splitting tensile strength.

Mixture ID	Average Compressive Strength 90 Days (MPa)	Average Splitting Tensile Strength	
		90 Days (MPa)	365 Days (MPa)
LS	2.4 ± 1.1	0.31 ± 0.05	0.60 ± 0.10
LS-G1	2.1 ± 0.2	0.33 ± 0.05	0.76 ± 0.13
LS-G2	3.3 ± 1.0	0.47 ± 0.25	0.79 ± 0.12
LF	2.3 ± 0.6	0.23 ± 0.04	0.45 ± 0.14
LF-G1	3.2 ± 0.8	0.28 ± 0.08	0.37 ± 0.02
LF-G2	3.2 ± 0.4	0.28 ± 0.09	0.43 ± 0.05

The average compressive strength of the tested grouts at the age of 90 days ranged from 2.1 to 3.3 MPa (Table 6). The comparison of grouts LF and LF-G1 shows that animal glue has some influence on increasing the average compressive strength by up to 39%, but in the case of grouts LS and LS-G1, the organic additive reduces considerably only the standard deviation of the compressive strength results, while the compressive strength itself does not change. In the study by Ventolà [12], the compressive strength of lime mortar with animal glue improves, which could be related to the acceleration of the carbonation process responsible for the transformation of portlandite into calcite. The same conclusions were drawn by Sickels [9], who found that animal glue as an additive has a positive effect on strength, which is consistent with our results of grout LF-G1 compared to the reference LF. In contrast to these studies, Elert et al. [13] showed that animal glue reduces compressive and flexural strength by up to 30–60% compared to lime plasters without organic additives. The higher the concentration of organic additive, the lower the measured strength. Elert et al. [13] attribute this effect to the delay in carbonization caused by the organic additive and the resulting large air bubbles, which can have a negative effect on the mechanical properties. According to Schellmann [22], animal glue can act as a foaming agent, leading to the formation of air bubbles during the mixing of grouts, which can reduce the strength. This effect of air bubbles could be a possible reason why the compressive strength of grout LS-G1 with animal glue did not increase compared to the reference grout LS.

Furthermore, all the tested grouts meet the requirements for lime-based repair mortars mentioned by Veiga [37], for which a compressive strength in the range of 0.4 to 2.5 MPa is recommended.

Grouts used to reattach detached plaster layers are generally expected to fail due to tensile stresses [6]. The differences between the results of splitting tensile strength are greater than those of compressive strength. At the ages of 90 and 365 days, the W/B ratio, animal glue, and the combination of F40 and F5 fillers are shown to have an effect on the average splitting tensile strength of the grouts. The animal glue in grouts LS-G1 and LF-G1 increases the average splitting tensile strength by 6% and 22%, respectively, compared to the reference grouts LS and LF with 0.31 and 0.23 MPa, respectively, at the age of 90 days. Moreover, the splitting tensile strengths increase after one year for all grouts. As mentioned above, the main reason for the higher strength could be the increased carbonation rate and the resulting lower porosity compared to 90-day-old grouts. The higher increase in the splitting tensile strength between 90 and 365 days for compositions with the animal glue is consistent with the results of total porosity (Figure 7) for LS-G1 and LF-G2 compositions. These results support the hypothesis that animal glue acts as a water-retention agent in the carbonation reaction [13,36].

In the tested grouts, particle packing plays an important role in cohesion and splitting tensile strength (grouts LS and LF). This requires the selection of a suitable size and proportion of the selected fillers to obtain an effective combination for optimum packing. From the results of the reference grouts LS and LF, it can be seen that the selected combination of the two fillers F40 and F5 is not optimal, as it reduces the splitting tensile strength. Moreover, grout LF contains a relatively high proportion of the large fraction <150 µm, which forms the basic skeleton in the structural matrix, and thus its voids may not be filled completely

by smaller particles of filler F5. Voids in the structural matrix reduce the strength of the grouts. In contrast, the particle size distribution of filler F15 is optimal, which is reflected in a higher splitting tensile strength.

The results show that the grouts of the first group (LS) with filler F15 reached the values for splitting tensile strengths of 0.3–1.2 MPa required by Ferragni et al. [38] already after 90 days, and all grouts fulfilled this requirement at the age of 365 days. These values at the age of 90 days are close to those proposed by Veiga [39] for plasters and repair mortar for historic buildings.

3.4. Adhesive Strength

Table 7 shows the pull-off strength with fracture type for the grouts injected into 2 mm and 5 mm air pockets before and after accelerated aging at the age of 1 year. The adhesive strength of the grouts was evaluated using the modified disc-sandwich model [32].

The adhesive strength of the grouts aged under laboratory conditions is lower than that of the grouts exposed to accelerated aging. The average values for normally aged grouts in 2 mm or 5 mm air pockets range from 0.07 to 0.15 MPa, i.e., they are 17–68% lower than the average values after accelerated aging.

When comparing the results of 2 mm and 5 mm air pockets, two opposite trends can be observed, depending on the height of the air pocket and the composition of the grout. For the normally aged grouts LS and LS-G2 with filler F15, the adhesive strength increases with the increasing thickness of the air pocket. In contrast, the adhesion strength for the thinner 2 mm air pocket is higher for the normally aged grouts LF and LF-G2 with fillers F40 and F5 than for the 5 mm air pockets. In addition, the pull-off strength is the same for the normally aged grouts LS-G1 and LF-G1 injected into 2 mm and 5 mm air pockets.

From the results in Table 7, it is not evident that animal glue improves the adhesive strength of the lime grout, which was shown in the study of [9]. One of the possible reasons could be the small content of the animal glue added to the grout in our study, since the adequate cohesion of the fresh grout was the key parameter for the animal-glue-dosage selection. On the other hand, the rate of lime grout carbonation inside the sandwich discs is much lower than that of cylindrical specimens (Figure 7).

Furthermore, the lower W/B ratio does not improve adhesion strength when we compare the normally aged reference specimens LS and LF with LS-G2 and LF-G2. For the 2 mm air pocket, the reference grouts (LS and LF) and grouts LS-G2 and LF-G2 with a low W/B ratio reach the values of 0.10 MPa and 0.15 MPa, respectively. The adhesion strengths for the 5 mm air pockets injected with grouts LS-G2 and LF-G2 decreased compared to the reference grouts LS and LF. From the water-retention results (Table 5), it can be seen that a lower W/B ratio increases the water retention of grouts LS-G2 and LF-G2, in contrast to grouts LS and LF. It is possible that the higher water-retention capacity of grouts LS-G2 and LF-G2 counteracts the release of water into the porous lime mortar, resulting in a reduced bond strength between the grout and plaster layer.

From the results of the rupture location of the grouts (Table 7), it is evident that the mixed fracture mode prevails partly along the interface between the grout and rough plaster and partly in the grout and rough plaster.

As mentioned in the study of [32], the effectiveness of the grouting process can be assessed from the injected area in the disc-sandwich system by the presence of voids that are not filled by the grout and by the presence of drying cracks formed in the grout. Voids and drying cracks were visible on the specimens after the pull-off test. It was observed that the grout did not completely fill the air voids because air bubbles formed during the grouting process (Figure 8). The grouts injected into the 2 mm and 5 mm air pockets contained up to 20% of voids in the grout structure (Table 7). In addition, drying cracks were visible in all grouts and were approximately less than 0.5 mm wide.

Table 7. Pull-off strength and location of failure before and after accelerated aging of grouts injected into 2 mm and 5 mm air pockets.

Mixture ID	2 mm (MPa)	Location of Failure	5 mm (MPa)	Location of Failure
LS	0.10 ± 0.01	80% along the grout–rough plaster interface 10% within the rough plaster 10% voids	0.15 ± 0.04	30% within the grout 50% along the grout–rough plaster interface 10% within the rough plaster 20% voids
LS 3% NaCl	0.24 ± 0.07	10% within the grout 80% within the rough plaster 10% voids	0.18 ± 0.07	5% along the grout–fine plaster interface 85% along the grout–rough plaster interface 10% voids
LS-G1	0.11 ± 0.06	90% along the grout–rough plaster interface 10% voids	0.10 ± 0.08	95% along the grout–rough plaster interface 5% voids
LS-G1 3% NaCl	0.25 ± 0.06	95% along the grout–rough plaster interface 5% voids	0.27 ± 0.14	80% within the grout 10% along the grout–rough plaster interface 10% voids
LS-G2	0.10 ± 0.06	90% along the grout–rough plaster interface 5% within the rough plaster 5% voids	0.12 ± 0.09	10% along the grout–fine plaster interface 10% within the grout 60% along the grout–rough plaster interface 20% voids
LS-G2 3% NaCl	0.24 ± 0.06	10% along the grout–fine plaster interface 80% within the grout 10% voids	0.20 ± 0.03	90% within the grout 10% voids
LF	0.15 ± 0.01	10% along the grout–fine plaster interface 50% within the grout 20% along the grout–rough plaster interface 20% voids	0.11 ± 0.02	10% within the grout 90% along the grout–rough plaster interface
LF 3% NaCl	0.26 ± 0.02	100% along the grout–rough plaster interface	0.28 ± 0.00	80% along the grout–fine plaster interface 5% within the grout 15% voids
LF-G1	0.11 ± 0.01	90% within the grout 10% voids	0.11 ± 0.01	30% along the grout–fine plaster interface 60% within the grout 10% voids
LF-G1 3% NaCl	0.26 ± 0.07	50% within the grout 30% along the grout–rough plaster interface 20% voids	0.12 ± 0.07	90% within the grout 10% voids
LF-G2	0.15 ± 0.09	40% within the grout 40% along the grout–rough plaster interface 20% voids	0.07 ± 0.06	80% within the grout 20% voids
LF-G2 3% NaCl	0.11 ± 0.04	90% within the grout 10% voids	0.20 ± 0.13	90% along the grout–fine plaster interface 10% voids



Figure 8. Disc-sandwich model after the adhesion test; grout LS injected into 5 mm air pocket.

The accelerated aging of the disc-sandwich specimens in the presence of de-icing salt (3% NaCl) showed that the grouts (LS, LS-G1, LS-G2, LF, LF-G1, and LF-G2) maintained (LF-G2) or even gained (the rest of the grouts under consideration) additional adhesive strength during exposure, although the cycles of freezing and thawing and heating and cooling are considered harmful for lime-based materials. From the results in Table 7, we can also conclude that the thickness of the air pocket may affect the resistance of the grout to accelerated aging. Grouts LS and LF-G1 injected into 5 mm-thick air pockets exhibit a lower resistance to freezing–thawing and heating–cooling cycles compared to the same grouts injected into 2 mm-thick air pockets. Padovnik and Bokan-Bosiljkov [1] reported that injection grout specimens with a similar composition to grout LS fell apart during testing due to the combined effect of water freezing and salt crystallization. In this study, the de-icing salt solution evaporated due to the capillary action of the lime plaster and the grout on the surface of the fine plaster where the salt crystallized; this effect occurred in all injected disc specimens (Figure 9a). It was found that the effect of capillary suction through the grout layer with the combination of wetting, freezing, and drying was most likely responsible for accelerating the carbonation of the lime binder and improving the adhesion strength of the grouts. Similar behavior was observed in [1].

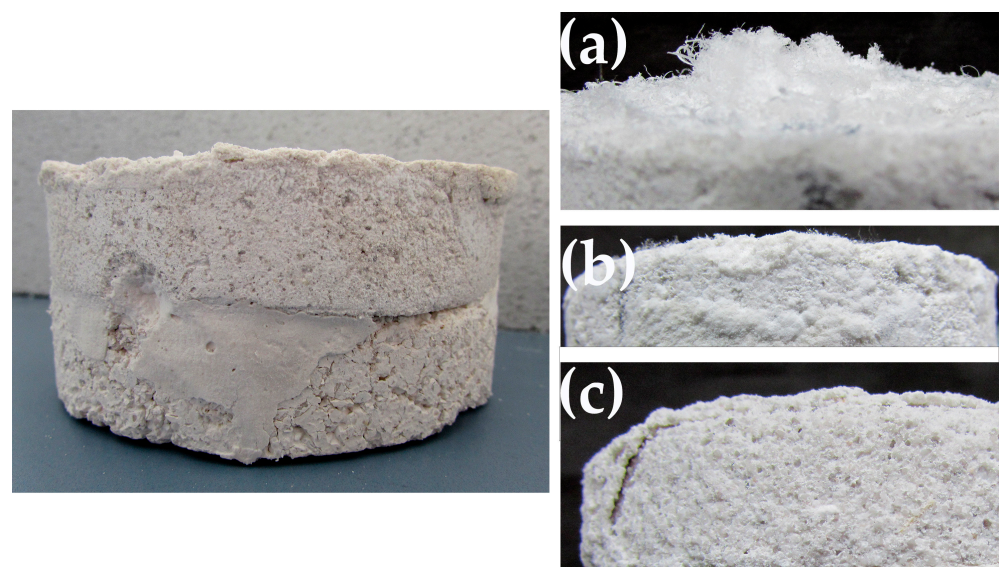


Figure 9. Disc-sandwich model (left) and typical damages (right) after accelerated aging: (a) salt crystallization on the plaster surface; (b) swelling and dusting; (c) formation of cracks and scaling.

In contrast, Elert et al. [13] report that the presence of animal glue improves the weathering resistance of carbonated plaster, which is not consistent with our results. Comparing the results of the reference grouts LS and LF with the grouts containing animal glue, it can be seen that animal glue has no significant effect on improving adhesive strength.

After 10 cycles of freezing–thawing and heating–cooling of the injected disc-sandwich system, dusting, swelling, scaling, and the formation of cracks appeared on the surface of the fine plaster (Figure 9). We can conclude that the tested grouts are a very durable solution that can consolidate detached decorative plasters when salts are present in the wall. The high durability of the grouts can also be attributed to the high total and capillary porosity (Figure 7) and the presence of air bubbles in the grout matrix.

The results in Table 7 cannot be directly compared with the pull-off strengths reported in other studies [1,5,32,40] because of the disc specimens' dimensions [32]. Further, the composition of the grout and plaster, the shape and thickness of the air pocket, and the curing time and conditions affect the test results [40]. However, these results show higher values than in other studies [1,5,40]. We believe that for lime-based materials that possess a low inherent strength, modified test methods such as those proposed in [34] should be used to test their adhesive strength, rather than the methods developed for cement-based materials.

4. Conclusions

In this study, the influence of organic additives and the different particle size distributions of fillers on the fresh and hardening properties of lime injection grouts was investigated. Fish glue was used as an organic additive to improve the cohesion of fresh grout and was found to be partially effective in improving other properties of the lime grouts, among them the compressive and splitting strength. This observation is not in agreement with a previous study [12], in which animal glue in lime plasters effectively improved their mechanical properties. However, the dosage of animal glue in [14] is much higher than that in our study, and this difference is most probably responsible for the different behavior of the studied specimens.

The addition of animal glue does not affect wet density and water-retention capacity, but it has a positive effect on fluidity for the composition with the F15 filler. The results of injectability show that the addition of animal glue increases the injection time compared to the reference grout and thus slows down the grouting process. It seems that the combination of fillers F40 and F5 and animal glue is beneficial when the injectability of the grout is addressed.

The combination of fillers F40 and F5 and animal glue increases the average 90-day compressive strength considerably, while for the composition with filler F15, this strength is maintained, compared to the reference composition without animal glue. The faster carbonation facilitated by animal glue is most probably responsible for the observed behavior. Faster carbonation in combination with the higher total and capillary porosity of the LS-G1 specimens compared to the LS specimens is responsible for the maintained compressive strength.

The results show that animal glue in lime grouts as a rule increases the splitting tensile strength compared to the reference grouts without traditional organic additives. For the 1-year-old specimens this is consistent with the porosity results, as the total and capillary porosity decreased by up to 15% compared to the 90-day-old samples. This is due to the presence of proteins in organic additives, which influence the carbonation reaction in the lime matrix and thus contribute to increasing the strength of lime grouts and consequently to reducing porosity [16]. However, the gradation of the filler also plays an important role when the increase in splitting tensile strength is addressed.

The combination of two fillers, F40 and F5, with a superior grading (with a wide range of particle sizes) improves the water retention and fluidity of the grout. Moreover, injectability is easier for compositions with the animal glue compared to those prepared with the F15 filler. This indicates that the packing density of the solid particles of the grouts

was effective and almost no water could be released in contact with the porous plaster. On the other hand, in compositions with a combination of the F40 and F5 fillers, the carbonation process may be slowed compared to those with the F15 filler, at least after 90 days of sample curing. Moreover, the F15 filler seems to increase splitting tensile strength considerably compared to the F40 and F5 combination.

The accelerated aging of the disc-sandwich models in the presence of de-icing salt (3% NaCl) showed that the grouts increase their resistance during the freezing–thawing and heating–cooling cycles. Most likely, the effect of capillary suction through the grout during the combination of wetting, freezing, and drying was responsible for the fastest carbonation process and the improvement of the adhesive strength of the grouts. These results highlight the importance of water in the carbonation process of the lime binder. Consequently, the adhesion and cohesion strengths of the grouts were as a rule considerably higher for the aged specimens than those of the non-aged specimens.

The results of this study suggest that most of the injection grouts studied may be used to stabilize detached decorative plaster layers that are not severely affected by moisture problems. Future research should address the potential risk of microbial deterioration associated with the organic animal glue in the grouts.

Author Contributions: Conceptualization, A.P. and V.B.-B.; methodology, A.P. and V.B.-B.; validation, V.B.-B.; formal analysis, A.P. and V.B.-B.; investigation, A.P.; resources, V.B.-B.; writing—original draft preparation, A.P.; writing—review and editing, V.B.-B.; visualization, A.P.; supervision, V.B.-B.; project administration, A.P.; funding acquisition, A.P. and V.B.-B. All authors have read and agreed to the published version of the manuscript.

Funding: This research was funded by the project C3330-17-529030 “Raziskovalci-2.0-UL-FGG-529030”. The Ministry of Education, Science and Sport of the Republic of Slovenia approved the project. The investment is co-financed by the Republic of Slovenia and the European Union under the European Regional Development Fund. The authors also acknowledge the financial support from the Slovenian Research Agency through the research core funding No. P2-0185.

Institutional Review Board Statement: Not applicable.

Informed Consent Statement: Not applicable.

Data Availability Statement: Data sharing is not applicable to this article.

Conflicts of Interest: The authors declare no conflict of interest.

References

1. Padovnik, A.; Bokan-Bosiljkov, V. Effect of Ultralight Filler on the Properties of Hydrated Lime Injection Grout for the Consolidation of Detached Historic Decorative Plasters. *Materials* **2020**, *13*, 3360. [CrossRef]
2. Pasion, C.; Piqué, F.; Jornet, A. Non-structural injection grouts with reduced water content: Changes induced by the partial substitution of water with alcohol. *Stud. Conserv.* **2017**, *62*, 43–54. [CrossRef]
3. Pasion, C.; Porter, J.H.; Gorodetska, M.; Parisi, S. Developing a Lime-Based Injection Grout with no Additives for Very Thin Delamination: The Role of Aggregates and Particle Size/Morphology. In *Conservation and Restoration of Historic Mortars and Masonry Structures*, 1st ed.; Bokan Bosiljkov, V., Padovnik, A., Turk, T., Eds.; Springer Nature: Cham, Switzerland, 2023; pp. 554–566.
4. Pasion, C.; Secco, M.; Piqué, F.; Artioli, G.; Rickerby, S.; Cather, S. Lime-based injection grouts with reduced water content: An assessment of the effects of the water-reducing agents ovalbumin and ethanol on the mineralogical evolution and properties of grouts. *J. Cult. Herit.* **2018**, *30*, 70–80. [CrossRef]
5. Azeiteiro, L.C.; Velosa, A.; Paiva, H.; Mantas, P.Q.; Ferreira, V.M.; Veiga, R. Development of grouts for consolidation of old renders. *Constr. Build. Mater.* **2014**, *50*, 352–360. [CrossRef]
6. Rainer, L.; Biçer-Şimşir, B. Evaluation of Lime-Based Hydraulic Injection Grouts for the Conservation of Architectural Surfaces. Los Angeles: Getty Conservation Institute. Available online: http://hdl.handle.net/10020/gci_pubs/evaluation_grouts (accessed on 8 November 2011).
7. Maravelaki, P.-N.; Kapetanaki, K.; Papayianni, I.; Ioannou, I.; Faria, P.; Alvarez, J.; Stefanidou, M.; Nunes, C.; Theodoridou, M.; Ferrara, L.; et al. RILEM TC 277-LHS report: Additives and admixtures for modern lime-based mortars. *Mater. Struct.* **2023**, *56*, 106. [CrossRef]
8. Centauro, I.; Cantisani, E.; Grandin, C.; Salvini, A.; Vettori, S. The Influence of Natural Organic Materials on the Properties of Traditional Lime-Based Mortars. *Int. J. Archit. Herit.* **2017**, *11*, 670–684. [CrossRef]

9. Sickels, L.-B. Organics vs. synthetics: Their use as additives in mortars. In *Mortars, Cements and Grouts Used in the Conservation of Historic Buildings*; ICCROM Symposium: Rome, Italy, 1982; pp. 25–52.
10. Pasion, C.; Secco, M.; Pique, F.; Rickerby, S.; Artioli, G.; Cather, S. Performance of grouts with reduced water content: The importance of porosity and related properties. In *Proceedings of the 4th Historic Mortars Conference—HMC 2016*, Santorini, Greece, 10–12 October 2016; Papayianni, I., Stefanidou, M., Pacht, V., Eds.; Laboratory of Building Materials, Department of Civil Engineering, Aristotle University of Thessaloniki: Thessaloniki, Greece, 2016; pp. 639–646.
11. Papayianni, I.; Karvounaris, T.; Pacht, V. Reattachment of a wall painting in a 16th century post-Byzantine church. In *Proceedings of the 4th Historic Mortars Conference—HMC 2016*, Santorini, Greece, 10–12 October 2016; Papayianni, I., Stefanidou, M., Pacht, V., Eds.; Laboratory of Building Materials, Department of Civil Engineering, Aristotle University of Thessaloniki: Thessaloniki, Greece, 2016; pp. 630–638.
12. Ventolà, L.; Vendrell, M.; Giraldez, P.; Merino, L. Traditional organic additives improve lime mortars: New old materials for restoration and building natural stone fabrics. *Constr. Build. Mater.* **2011**, *25*, 3313–3318. [[CrossRef](#)]
13. Elert, K.; García Sánchez, R.M.; Benavides-Reyes, C.; Linares Ordóñez, F. Influence of animal glue on mineralogy, strength and weathering resistance of lime plasters. *Constr. Build. Mater.* **2019**, *226*, 625–635. [[CrossRef](#)]
14. Jayasingh, S.; Selvaraj, T.; Raneri, S. Evaluating the Impact of Organic Addition and Aggregate Gradation on Air Lime Mortar: New Compatible Green Material for Heritage Application. *Int. J. Archit. Herit.* **2022**, *16*, 681–691. [[CrossRef](#)]
15. Ravi, R.; Rajesh, M.; Thirumalini, S. Mechanical and physical properties of natural additive dispersed lime. *J. Build. Eng.* **2018**, *15*, 70–77. [[CrossRef](#)]
16. Jayasingh, S.; Selvaraj, T. Influence of organic additive on carbonation of air lime mortar—Changes in mechanical and mineralogical characteristics. *Eur. J. Environ. Civ. Eng.* **2020**, *26*, 1776–1791. [[CrossRef](#)]
17. Stefanidou, M.; Papayianni, I. The role of aggregates on the structure and properties of lime mortars. *Cem. Concr. Compos.* **2005**, *27*, 914–919. [[CrossRef](#)]
18. Nogueira, R.; Ferreira Pinto, A.P.; Gomes, A. Design and behavior of traditional lime-based plasters and renders. Review and critical appraisal of strengths and weaknesses. *Cem. Concr. Compos.* **2018**, *89*, 192–204. [[CrossRef](#)]
19. Pavía, S.; Toomey, A.B.; Toomey, Á.B. Influence of the aggregate quality on the physical properties of natural feebly-hydraulic lime mortars. *Mater. Struct.* **2008**, *41*, 559–569. [[CrossRef](#)]
20. *UNI EN 459-1*; Building Lime—Part 1: Definitions, Specifications and Conformity Criteria. CEN: Brussels, Belgium, 2010.
21. *UNI EN 459-2*; Building Lime—Part 2: Test Methods. CEN: Brussels, Belgium, 2010.
22. Schellmann, N.C. Animal glues: A review of their key properties relevant to conservation. *Stud. Conserv.* **2007**, *52*, 55–66. [[CrossRef](#)]
23. Fish Glue Solution, Deffner&Johann. Available online: https://deffner-johann.de/pub/media/datasheets/2416000/EN/2416000_Technical%20Data%20Sheet_Fish%20Glue%20Solution%20Liquid_EN_DJ.pdf (accessed on 25 May 2019).
24. Derrick, R.M.; Stulik, C.D.; Landry, M.J. *Infrared Spectroscopy in Conservation Science*; J. Paul Getty Trust: Los Angeles, CA, USA, 1999; p. 181.
25. *EN 1015-6*; Methods of Test for Mortar for Masonry, Part 6: Determination of Bulk Density of Fresh Mortar. CEN: Brussels, Belgium, 1999.
26. *PrEN 1015-8*; Methods of Test for Mortar for Masonry, Part 8: Determination of Water Retentivity of Fresh Mortar. CEN: Brussels, Belgium, 1999.
27. *EN 445*; Grout for Prestressing Tendons—Test Methods. CEN: Brussels, Belgium, 2007.
28. *EN 1771*; Products and Systems for the Protection and Repair of Concrete Structures, Test Methods—Determination of Injectability and Splitting Test. CEN: Brussels, Belgium, 2004.
29. *SIA 262/1*; Construction En Béton—Spécifications Complémentaires, Appendix A. SIA: Zurich, Switzerland, 2008.
30. *EN 1015-11*; Methods of Test for Mortar for Masonry, Part 11: Determination of Flexural and Compressive Strength of Hardened Mortar. CEN: Brussels, Belgium, 1999.
31. *ASTM C496/C496M-1*; Standard Test Method for Splitting Tensile Strength of Cylindrical Concrete Specimens. ASTM International: Harrisburg, PA, USA, 2004.
32. Padovnik, A.; Bokan Bosiljkov, V. Adhesive-strength assessment of lime injection grout using standardised and modified test methods. *Mater. Technol.* **2022**, *56*, 587–593. [[CrossRef](#)]
33. *EN 1015-12*; Methods of Test for Mortar for Masonry—Part 12: Determination of Adhesive Strength of Hardened Rendering and Plastering Mortars on Substrates. CEN: Brussels, Belgium, 2001.
34. RILEM TC 25-PEM. Test No. II. 6, Water absorption coefficient. *Mater. Struct.* **1980**, *13*, 209.
35. Ince, C.; Ozturk, Y.; Carter, M.A.; Wilson, M.A. The influence of supplementary cementing materials on water retaining characteristics of hydrated lime and cement mortars in masonry construction. *Mater. Struct.* **2014**, *47*, 493–501. [[CrossRef](#)]
36. Walker, R.; Pavía, S. The impact of water retainers in hemp-lime concrete with pozzolans. *J. Build. Limes Forum* **2013**, *20*, 12–20.
37. Veiga, R. Air lime mortars: What else do we need to know to apply them in conservation and rehabilitation interventions? A review. *Constr. Build. Mater.* **2017**, *157*, 132–140. [[CrossRef](#)]
38. Ferragni, D.; Forti, M.; Malliet, J.; Mora, P.; Teutonico, J.M.; Torraca, G. Injection grouting of mural paintings and mosaics. *Stud. Conserv.* **1984**, *29*, 110–116. [[CrossRef](#)]

39. Veiga, R. Conservation of Historic Renders and Plasters: From Laboratory to Site. In *Historic Mortars*; Válek, J., Hughes, J.J., Groot, C.J.W.P., Eds.; RILEM Bookseries; Springer: Dordrecht, The Netherlands, 2012; Volume 7, pp. 207–225.
40. Pasian, C.; Piqué, F.; Jornet, A.; Cather, S. A ‘Sandwich’ Specimen Preparation and Testing Procedure for the Evaluation of Non-Structural Injection Grouts for the Re-Adhesion of Historic Plasters. *Int. J. Archit. Herit.* **2019**, *15*, 445–466. [[CrossRef](#)]

Disclaimer/Publisher’s Note: The statements, opinions and data contained in all publications are solely those of the individual author(s) and contributor(s) and not of MDPI and/or the editor(s). MDPI and/or the editor(s) disclaim responsibility for any injury to people or property resulting from any ideas, methods, instructions or products referred to in the content.